Macromol. Symp. ***190***, *161–172 (2002)*

Structure and Ordering Kinetics of Micelles in Triblock Copolymer Solutions in Selective Solvents

*R. Bansil** [1], *H. Nie* [1], *Y. Li* [1], *G. Liao* [1], *K. Ludwig* [1], *M. Steinhart* [2], *Č. Koňák* [2], *J. Lal* [3]

[1] Department of Physics, Boston University, Boston, MA 02215. USA
[2] Institute of Macromolecular Chemistry, Academy of Sciences of the Czech Republic, 162 06 Prague 6, Czech Republic
[3] Argonne National Laboratory, Argonne, Illinois, USA

SUMMARY: We have used small-angle x-ray scattering (SAXS), and small-angle neutron scattering (SANS) to study the micelle structure of a polystyrene-*block*-poly(ethene-*co*-butene)-*block*-polystyrene triblock copolymer in dilute - semidilute solutions in solvents selective for either the outer styrene block (dioxane) or for the middle block (heptane or tetradecane). Measurements of equilibrium structure factors showed that micelles were formed in both types of selective solvents. In the case of dioxane, the micelles are isolated whereas in the case of heptane or tetradecane, a bridged micellar structure may be formed at higher copolymer concentrations. In both cases we observed an ordered cubic structure of insoluble domains (micellar cores) at high concentrations (> 8 %). The micellar scattering function was fit to the Percus-Yevick interacting hard-sphere model. The temperature dependence of the core radius, the hard-sphere interaction radius and the volume fraction of hard spheres were obtained. We also used synchrotron-based time-resolved SAXS to examine the kinetics of ordering of the micelles on a cubic lattice for many different temperature jumps into the ordered cubic phase starting from the disordered micellar fluid phase in different solvents at different concentrations. The time evolution of the structure changes was determined by fitting the data with Gaussians to describe the structure factor of the ordered Bragg peaks and the Percus-Yevick structure factor was used to describe the micellar fluid. The time dependence of the peak intensities and widths as well as of the micellar parameters will be presented. The results showing the kinetics of the transformation from the fluid to the ordered phase were analyzed using the Mehl-Johnson-Avrami theory of nucleation.

INTRODUCTION

The structure and properties of block copolymers have attracted much interest recently.[1,2] It is well known that, in a selective solvent which preferentially solubilizes one of the chemical components, the insoluble polymer blocks of both di- and triblock copolymers form micelles.[2] These micelles are also known to exhibit a transition between a liquid-like state and an ordered solid-like state at higher copolymer concentrations.[3-5] In the liquid-like structure, the

 CCC 1022-1360/00/$ 17,50+.50/0

positions of micelles do not exhibit any long-range spatial order, but show a similar short-range order to that in a liquid.

The thermodynamics of micelle formation and structures in diblock copolymer is well understood.[6-10] Recently a few studies have investigated the structure of micelles and their ordering in triblock copolymer solutions.[3,11-13] In the case of symmetric triblocks (ABA), the morphology of the micelles depends on whether the solvent solubilizes the outer (A) or the inner (B) block, leading to the formation of either isolated or bridged micelles, respectively.[12] Lodge et al[13] have used small-angle x-ray scattering (SAXS) to investigate the structure of polystyrene-*block*-polyisoprene-*block*-polystyrene triblock copolymer in a selective solvent good for the outer block, while Raspaud et al[11] have used small-angle neutron scattering (SANS) to study a similar triblock copolymer in a selective solvent good for the middle block. Raspaud et al[11] found that the network formed by the outer blocks has a cubic-ordered structure at high concentrations. The cubic structure was also observed on the polystyrene-*block*-poly(ethene-*co*-butene)-*block*-polystyrene copolymer in a selective solvent good for the middle block by Kleppinger et al.[3] Understanding of the kinetics of micelle formation and of micellar ordering is not as advanced as of the equilibrium copolymer structures, despite the obvious fundamental and practical interest in this question. A few detailed studies on the kinetics of the ordering process in the diblock copolymers have been reported.[4,14-17] Temperature ramp measurements on triblock copolymers have been reported, along with some measurements of temperature jump kinetics. No detailed analysis of kinetics in these systems has been reported.

In this paper we present the results of SANS and a time-resolved SAXS study of the micelle structure and kinetics of the ordering process in the triblock copolymer polystyrene (S)-*block*-poly(ethene-*co*-butene) (EB)-*block*-polystyrene in the selective solvents, tetradecane, heptane and dioxane. Tetradecane and heptane are good solvents for the middle EB block, while dioxane is good for the outer S blocks.

EXPERIMENTAL

Block copolymer

The sample of S-EB-S block copolymer (Shell Chemicals, Kraton G1650) was fractionated and the middle fraction corresponding to 15 wt % of the raw sample, was used in this study. The molecular weight M_w of the fraction was 70,000 with polydispersity M_w/M_n= 1.05, and the styrene block content was 28 wt %.[18] This sample fraction was used in an earlier room temperature SAXS, light scattering and rheological studies.[18,19] Solutions ranging in concentration from 4 to 7 wt % were prepared by direct dissolution in the solvent around 90 °C. Higher concentrations were prepared by evaporating the solvent from the 7-% sample. Two kinds of deuterated solvents were used in the SANS study: heptane-d_{16}, and dioxane-d_8.

Small-angle X-ray scattering (SAXS)

The copolymer solutions were sealed between two thin flat Kapton windows glued to aluminum plates separated by an O-ring of diameter 1 cm. The SAXS measurements were performed at the X-20C beamline of the National Synchrotron Light Source at Brookhaven National Laboratory using a high-flux multilayer monochromator and a position-sensitive detector. The photon energy was 6.9 keV, which corresponds to a wavelength λ = 1.8 Å. The detector was positioned approximately 100 cm away from the sample to obtain a scattering vector range of 0.005 - 0.08 Å^{-1} . The absolute incident beam intensity was monitored with a helium-filled ion chamber. The background scattering from an empty Kapton cell was subtracted from the total scattering and the scattering intensities were normalized to an absolute scale per monomer unit using the ion-chamber current to correct for any change of the incident beam intensity or the sample absorption.

Small-angle neutron scattering (SANS)

Neutron scattering experiments were conducted at the small-angle neutron diffractometers at the intense pulsed neutron source, Argonne National Laboratory[20]. Neutrons with wavelengths 0.9-14 Å were used to cover the scattering vector range q = 0.005-0.35 Å^{-1}. The block copolymer solutions were maintained at constant temperature in a custom-designed demountable quartz cells with a path length of 1 mm. Further details of the time-of-flight instrument used can be found in literature.[20]

THEORETICAL MODEL FOR MICELLE SOLUTIONS

For a monodisperse system of particles, the scattering function can be written as a product of the single-particle form factor $P(q)$ and a structure factor $S(q)$, describing the interparticle interference:

$$I(q) = KNP(q)S(q) \tag{1}$$

where K is the contrast factor and N is the number density of scatterers. The form factor of a hard sphere with radius R_c can be written as

$$P(q) = v_0^2\Phi^2(qR_c) \tag{2}$$

where $v_0 = (4/3)\pi R_c^3$, is the volume of the hard sphere and

$$\Phi(x) = \frac{3}{x^3}(\sin x - x\cos x). \tag{3}$$

The Percus-Yevick hard-sphere structure factor is given by [21, 22]

$$S(q) = \frac{1}{1 + 24\phi G(2qR_{hs})/(2qR_{hs})}. \tag{4}$$

Here $\phi = 4/3\pi R_{hs}^3 N$ is the hard-sphere volume fraction, R_{hs} being the hard-sphere interaction radius and

$$G(x) = \frac{\alpha}{x^2}(\sin x - x\cos x) + \frac{\beta}{x^3}[2x\sin x + (2 - x^2)\cos x - 2]$$
$$+ \frac{\gamma}{x^5}\{-x^4\cos x + 4[(3x^2 - 6)\cos x + (x^3 - 6x)\sin x + 6]\} \tag{5}$$

Thus the scattering intensity is a function of the hard-sphere volume fraction ϕ, the core radius R_c and the hard-sphere interaction radius R_{hs}. These parameters can be obtained by the least-square fitting of the scattering intensity data to Eqs. 1-5.

RESULTS AND DISCUSSION

Equilibrium structure of semidilute triblock copolymer solutions

Static scattering measurements were made with both SANS and SAXS techniques, as a function of temperature, concentration and solvent. Typical results are discussed below.

Temperature dependence

Figure 1 shows the scattering intensity from 7-wt % S-EB-S solution in tetradecane at different temperatures. At 90° C, the scattering intensity $I(q)$ is featureless, implying that micelles are not formed at this temperature. Below 80 °C, $I(q)$ shows one well-formed maximum in the structure factor at low q values near 0.018 Å^{-1}. In addition, a shoulder is discernible near 0.03 Å^{-1}, which becomes more pronounced as the temperature decreases. This scattering behavior originates from the short-range ordering of micelle cores formed by the insoluble S blocks and can be described by the Percus-Yevick hard-sphere model.[21,22] Similar scattering behavior has been observed in many block copolymer micellar systems.[3,5,11,13,17,21] The solid lines in Fig. 1 show the fitted result. The fit works well around the peak at $q \approx 0.018$ Å. For the values beyond the shoulder, significant deviation from the hard-sphere approximation is observed. This may indicate that, although the hard-sphere interaction radius R_{hs} is well defined, the micelles do not have sharp surfaces. Moreover, the data at higher

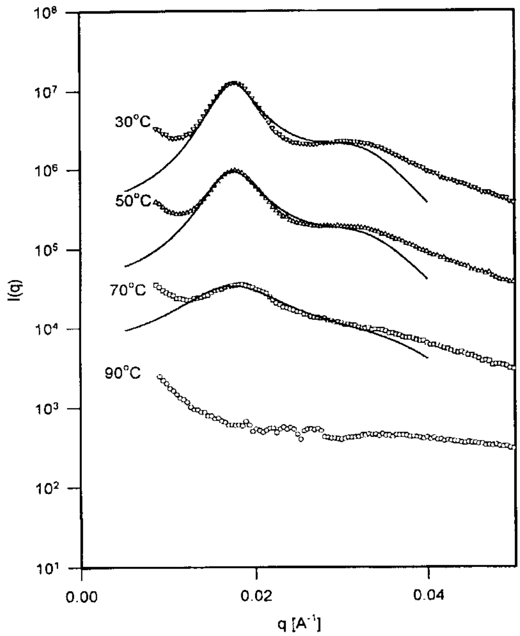

Figure 1. The scattering intensity $I(q)$ versus q from 7-wt % solution in tetradecane at different temperatures. The data are offset by factors of 10 for clarity. The solid lines are fit to the Percus-Yevick hard-sphere model.

q's can be better described by introducing a Gaussian distribution of R_c[23] to reflect the polydispersity in droplet size distribution. For the fitting parameters presented below, we have restricted fitting to the q range from $q_0/2$ to $2q_0$ and polydispersity effects of R_c are not included in the fit.

From the fits we obtained information on the micellar core radius, hard-sphere interaction radius and hard-sphere volume fraction as a function of temperature. The results are shown in Fig. 2. The micellar core radius R_c and the hard-sphere radius R_{hs} both increase as the temperature decreases below 80 °C. This probably reflects changes in the aggregation number of micelles but can also be partly due to the change in micelle size due to conformational changes of the polymer chains. Below 40 °C, both R_c and R_{hs} appear to saturate, and show a very small temperature dependence. Similar temperature dependences of R_c and R_{hs} were observed in other triblock copolymer solutions.[5] The core radius increases from approximately 76 Å at 80 °C to 86 Å at 40 °C; the hard-sphere interaction radius increases from 160 Å at 80 °C to 188 Å at 40 °C.

Since tetradecane is a poor solvent for the outer S blocks and good solvent for the middle EB blocks, two possible micellar structures can be formed. One possibility is that the micelles formed by the end S blocks are bridged by the middle EB blocks so that the system behaves as

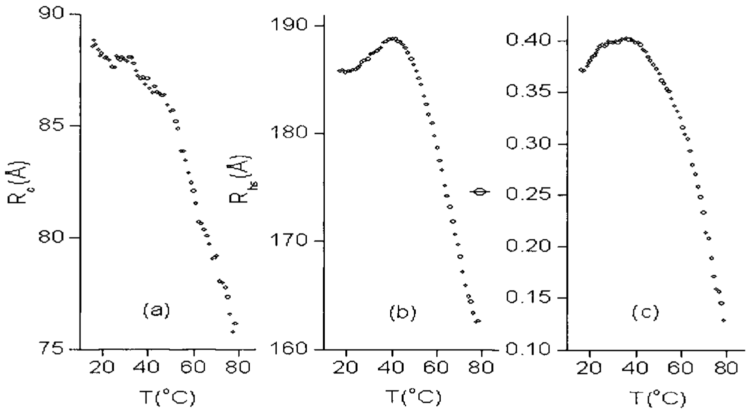

Figure 2. The temperature dependences of the micellar parameters for 7-wt% S-EB-S in tetradecane: (a) the core radius, R_c, (b) the hard-sphere interaction radius, R_{hs} and (c) the hard-sphere volume fraction, ϕ.

a polymer gel. The other possibility is that the middle blocks fold up in one micelle forming isolated flower-like micelles. Although the exact relations between R_c, R_{hs}, the segment length b, and the degree of polymerization N of polymer chains are unknown, in the case of bridged micelles we can estimate R_{hs} as half of the sum of the S and EB chain length. Taking the segment length b of the EB polymer and S polymer as 4.9 Å and 6.8 Å, respectively[24], and assuming the polymer chain is described as a random walk, we obtain that the length of EB chain in the good solvent (self-avoiding random walk) is $bN^{0.6}$ = 294 Å and the length of the S chain in the poor solvent (Gaussian chain) is $bN^{0.5}$ = 66 Å using the degree of polymerizations, N, for the EB chain 918 and for the S chain 94. This gives R_{hs} as 180 Å, consistent with the value obtained by fitting the data. We cannot say which structure is formed in the sample by our SAXS measurements. However, the interconnected structure was found to be favored in the rheological study on the same sample.[19]

Compared with R_c and R_{hs}, the volume fraction of hard spheres is more sensitive to the change of temperature as shown in Fig. 2c. The volume fraction ϕ increases from 0.12 at 80 °C to 0.4 at 40 °C. The increase in ϕ, R_{hs} and R_c is due to the fact that the outer S chains become less soluble with the decrease in temperature. Insoluble chains can be added to the existing micelles, causing the increase in hard-sphere radius R_c and thus R_{hs}, and/or the formation of new micelles, increasing the number of micelles per unit volume. At temperatures higher than 60 °C, the increase in the number of micelles dominates the increase in the hard-sphere volume fraction, since the increase in the volume of one hard sphere $v_{hs} = 4/3\pi R_{hs}^3$ is small compared with the increase in ϕ as easily seen in Fig. 2c. However, in the temperature region between 40 °C and 60 °C, the increase in R_{hs} is the main contributor to the increase in ϕ. Below 40 °C, ϕ saturates. This saturated value $\phi_0 \approx 0.4$ may correspond to the situation that all S chains are aggregated in micelles. In this situation, the aggregation number of S chains N_m in a micelle can be calculated from ϕ_0 and the corresponding R_{hs} by the relation[5]

$$N_m \phi_0 / (4/3\pi R_{hs}^3) = 2cN_A / M_w \tag{6}$$

where c is the concentration of the sample, N_A is Avogadro number and M_w is the molecular weight of the copolymer. The factor 2 is due to the fact that there are two S chains in a triblock copolymer. Taking R_{hs} = 188 Å, ϕ_0 = 0.4 at 40 °C, c = 0.07 g/cm^3, M_w = 70,000, we obtain N = 84.

The aggregation number N_m can also be obtained from the core radius R_c. If we assume the micelle core is considered as a condensed sphere consisting of only S chains, then

$$N_m V_S = (4/3)\pi R_c^3 \tag{7}$$

where $V_S = M_S / (\rho_S N_A)$ is the volume of a S chain, M_S = 9,800 is the molecular weight of S chain of our sample and ρ_S= 1.05 g/cm^3 is the mass density of S. This leads to N_m ranging from approximately 120 at 75 °C to 185 at 40 °C, which is twice as large as that obtained from the previous calculation, implying that the micelle cannot be a condensed sphere formed by only S chains. The presence of some solvent in the micelle core was also suggested in previous light scattering studies of the same sample.[25]

Similar results were obtained for the 7-wt % heptane solution of the sample. We did not observe an ordered structure of micelles either in the 7-wt % heptane or in 7-wt % tetradecane solution of the sample. Mortensen et al[26] found that ϕ_{hs} = 0.47 is the lower boundary for the existence of an ordered cubic arrangement of spherical microdomains. In both samples, the maximum value for ϕ we obtained is 0.4, lower than 0.47. This may explain why no ordered structure was observed in these samples. However, in the 15-wt % sample solution (discussed later), we obtained ϕ larger than 0.47 and observed a clear cubic structure.

Concentration and solvent dependence

Samples with different concentrations (4 - 15%) were studied at different temperatures from 25 °C to 90 °C in both the SAXS and the SANS experiments. Shown in Fig. 3 are SANS results at T = 25 °C for two concentrations in both the solvents.

A comparison of the two solvents shows that the interaction between micelles, characterized by the main peak in the scattering data, is stronger in heptane samples (bridged or flower-like micelles) than in the dioxane samples (isolated micelles). In the 4% sample, the micelles are not bridged, in either solvent. Details of fitting of these data to hard-sphere as well as core-shell models will be discussed elsewhere. In the 15% sample, the SAXS data clearly show the presence of Bragg peaks, indicating a cubic-ordered structure. The somewhat poorer resolution of the SANS data, makes it harder to see these features clearly from the SANS data, shown in Fig. 3.

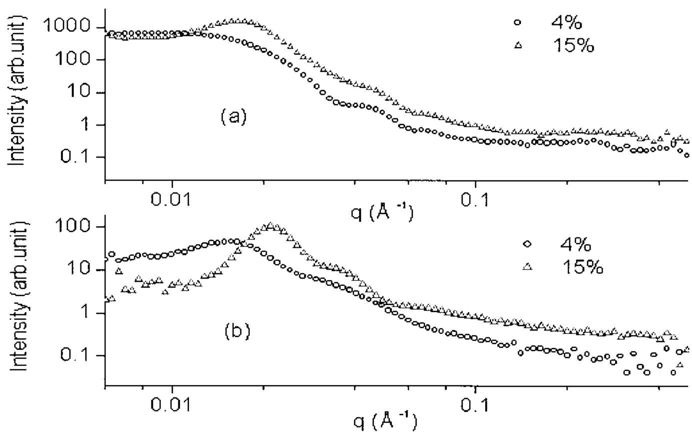

Figure 3. The SANS scattering intensity $I(q)$ versus q for 4-wt% and 15-wt % solution (a) in dioxane-d_8; (b) in heptane-d_{16} at 25 °C.

Ordering kinetics of the micelles in semidilute solutions selective for the middle block

The kinetics of the formation of the ordered micellar phase in a 15% S-EB-S solution in heptane was examined by SAXS measurements performed in a time-resolved way by averaging the scattered intensity on a position-sensitive detector camera for short durations (1 s or less) and repeating the measurements for periods up to 1 h.

Shown in Fig. 4 is the time evolution of the scattered intensity following a quench from 90 °C to 40 °C. The temperature became stable at 45 s after the quench. The scattering patterns during the first 45 s are characteristic of scattering from interacting hard-sphere and can be described by the Percus-Yevick model. After 45 s, well defined sharp peaks developed, signaling the formation of a long-range order. The relative positions of four observed peaks are approximately $1:\sqrt{2}:\sqrt{3}:2$, clearly revealing a cubic structure, either a simple cubic (sc) or a body-centered cubic (bcc) structure. The scattering from these Bragg peaks can be represented

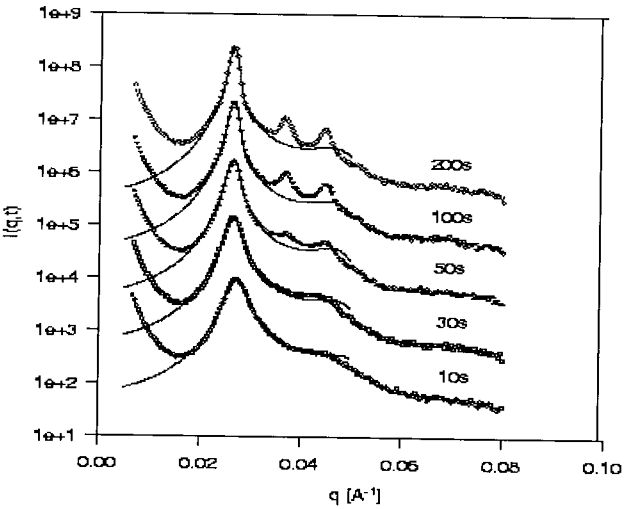

Figure 4. The scattering intensity from a 15% S-EB-S solution in heptane at different times following a quench from 90 °C to 40 ° C. The data are offset by factors of 10 for clarity. The scattering data around the first Bragg peak was fit by Eq. 8 (only i =1 term was included). The q region chosen for the fit was from 0.02 Å^{-1} to 0.035 Å^{-1}. The curves calculated from the fitted parameters are plotted as the solid lines.

by a Gaussian. The observed scattering $I(q,t)$ is then made up of two components:

$$I(q,t) = I_{\text{hs}}(q,t) + \sum_i A_i(t) \mathrm{e}^{-\frac{1}{2}\left(\frac{q-b_i}{\sigma_i}\right)^2} \tag{8}$$

where $I_{\text{hs}}(q,t)$, given by Eq. 1, is the scattering due to the hard spheres, and A_i , b_i , σ_i are the amplitude, position and peak width of the i-th Bragg peak, respectively. The scattering data around the first Bragg peak was fit by Eq. 8 (only i =1 term was included). The q region chosen for the fit was from 0.02 Å^{-1} to 0.035 Å^{-1} . The curves calculated from the fitted parameters are plotted as the solid lines in Fig. 4. Full details of fits with all three Gaussians included will be discussed in future publications.

Figure 5 shows the peak intensity of the three Bragg peaks of Fig. 4. The change of temperature with time is also included in Fig. 5. The appearance of the second Bragg peak indicates that the system starts an ordering process. While the micelle formation starts rapidly as the temperature is lowered, the ordering process occurs at a much later time. The same behavior was observed in a diblock copolymer in the selective solvent (Fig. 2 in [4]), suggesting that the kinetics of the ordering process in the triblock copolymer is similar to that in the diblock copolymer.

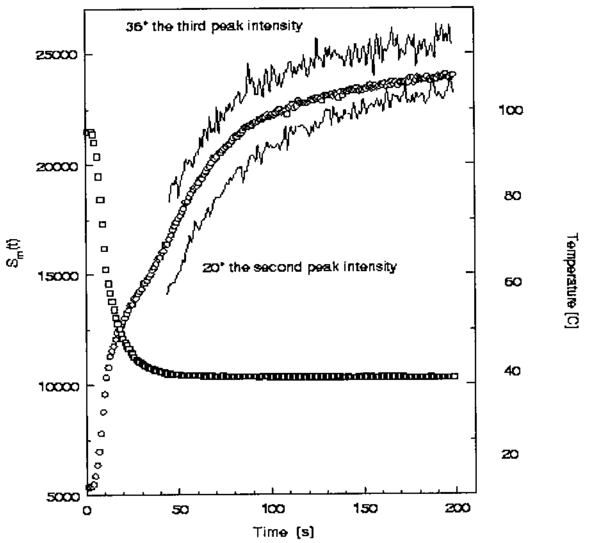

Figure 5. The peak intensities of the three Bragg peaks and temperature versus time. The appearance of the second Bragg peak indicates that the system starts an ordering process.

Figure 6 shows the fitted intensity of first-order Bragg peak, A_1(t) as a function of time following the quench. The first-order Bragg peak $A_1(t)$ is proportional to the fraction of material in the cubic-ordered state. Thus we can compare our experimental result with the nucleation theory prediction of the relation between the fraction of the assembly transformed as a function of time at constant temperature.

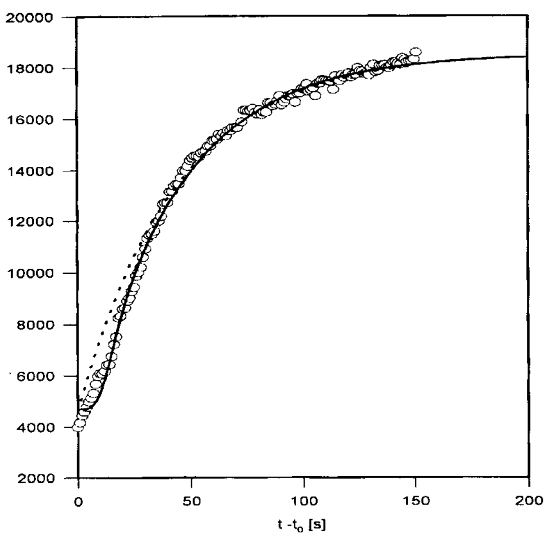

Figure 6. The fitted intensity of first-order Bragg peak, $A_1(t)$ as a function of time following the quench. The dotted line is fit to Eq. 9 and the solid line to Eq. 10.

For the nucleation and growth reaction, Johnson, Mehl and Avrami developed a transformation theory.[27] The theory predicts that for a three-dimensional nucleation and growth process, the volume fraction of the transformed phase η, should be

$$\eta = 1 - e^{-kt^{n}} \tag{9}$$

where $3 < n < 4$, k is a constant. Letting $A_1(t) = A_1(0) + [A_1(\infty) - A_1(0)]\eta$, we fit the first Gaussian intensity to Eq. 9. The dotted line in Fig. 6 is the result of the fit, giving $n \approx 1$. Cahn[27,28] derived a theory which describes nucleation occurring on two-dimensional defects. Cahn's theory includes the effect of impingement from different boundaries and assumes that the planar boundaries are randomly distributed in space. According to Cahn's theory, the volume fraction of the transformed phase can be written:

$$\eta = 1 - \exp(-bf(t - t_0)) \tag{10}$$

where $$f(t) = (t/a)\int_0^1 \{1 - \exp[-\frac{\pi}{3}(t/a)^3(1 - 3\xi^2 - 2\xi^3)]\}\,d\xi \tag{11}$$

and a and b are time constants related with the isotropic growth rates and nucleation rates. Both rates are assumed to be constant. In the early time, $f(t) \sim t^4$; at later times, $f(t) \sim t$. The direct fit of this model to the data with variable parameters a, b, I_0 and I_∞ is shown by the solid line in Fig. 6. The model fits the data better than Eq. 9. From Eqs. 10 and 11, it can be seen that the quantity $\tau = a/b$ plays the role of an effective time constant at the late time limit.[4,14] In the quench shown in Fig. 6, τ = 42.4 s. We do not know the physical origin of two-dimensional defects inherent in Cahn's treatment of the ordering process. Singh et al [14] argued that the likeliest source appears to be due to anisotropic, solid impurities incorporated into the samples.

CONCLUSION

In conclusion, we performed SANS and SAXS study on the micelle structure and the kinetics of the ordering process of S-EB-S triblock copolymer in semidilute solutions of selective solvents. Our results showed that in heptane or tetradecane, a solvent selective for the middle block, the scattering function can be fit by the Percus-Yevick hard-sphere model. The core radius, the hard-sphere interaction radius and the volume fraction of hard spheres increase and then saturate as the temperature decreases. The bridged micellar structure may be formed. In the opposite case of S-EB-S in dioxane, a solvent good for the outer S blocks, only isolated micelles were formed. At higher concentrations, we were able to observe a simple cubic structure of cores. The kinetics of the disorder-order transition following a quench of the temperature from 90 °C to 40 °C was measured, and qualitatively similar results to those observed in previous studies with diblock copolymer solutions were obtained. The results could be described by the classic nucleation and growth theory.

ACKNOWLEDGEMENT

This work was funded by the NSF U.S.-Czech Collaborative Research Grants (NSF INT-9600679 and ME CR ES 044). R.B. acknowledges the support of NSF, Division of Materials Research (NSF-DMR No. 9618467). C.K. and M.S. acknowledge the financial support of the Grant Agency of the Academy of Sciences of the Czech Republic (No. A1050201) and of the Grant Agency of the Czech Republic (No. 203/00/1317).

REFERENCES

[1] Bates, F.S.; Fredrickson, G.H. *Annu. Rev. Phys. Chem.* **1990**, *41*, 525.
[2] Tuzar, Z.; Kratochvil, P. *Surf. Colloid Sci.* **1992**, *15*, 1.
[3] Kleppinger, R.; Reynders, K.; Mischenko, N.; Overbergh, N.; John, M.H.J.; Mortensen K.; Reynaers, H. *Macromolecules* **1997**, *30*, 7008.
[4] Harkless, C.R.; Singh, M.A.; Nagler, S.E.; Stephenson, G.B.; Jordan-Sweet, J.L. *Phys. Rev. Lett.* **1990**, *64*, 2285.
[5] Mortensen, K.; Pedersen, J.S. *Macromolecules* **1993**, *26*, 805.
[6] Leibler, L. *Macromolecules* **1980**, *13*, 1602.
[7] Fredrickson, G.H.; Helfand, E. *J. Chem. Phys.* **1987**, *87*, 697.
[8] Shibayama, M.; Hashimoto, T.; Kawai, H. *Macromolecules* **1983**, *16*, 16.
[9] Stuhn, B.; Mutter, R.; Albrecht, T. *Europhys. Lett.* **1992**, *18*, 427.
[10] Almdal, K.; Bates, F.S. *J. Chem. Phys.* **1992**, *96*, 9122.
[11] Raspaud, E.; Lairez, D.; Adam, M.; Carton, J.-P. *Macromolecules* **1994**, *27*, 2956 *Macromolecules* **1996**, *29*, 1269.
[12] Balsara, N.P.; Tirrell, M.; Lodge, T.P. *Macromolecules* **1992**, *24*, 1973.
[13] Lodge, T.P.; Xu, X.; Ryu, C.Y.; Hamley, I.W.; Fairclough, J.R.A.; Ryan, A.J.; Pedersen, J.S. *Macromolecules* **1996**, *29*, 5955
[14] Singh, M.A.; Harkless, C.R.; Nagler, S.E.; Shannon, R.F.; Ghosh, S.S. *Phys. Rev. B* **1993**, *47*, 8425.
[15] Hashimoto, T.; Sakamoto, N.; Koga, T. *Phys. Rev. E* **1996**, *54*, 5832.
[16] Hashimoto, T.; Sakamoto, T. *Macromolecules* **1995**, *28*, 4779.
[17] Adams, J.L.; Quiram, D.J.; Graessley, W.W.; Register, R.A.; Marchand, G.R. *Macromolecules* **1996**, *29*, 2929.
[18] Plestil, J.; Hlavata, D.; Hrouz J.; Tuzar, Z. *Polymer* **1990**, *31*, 2112.
[19] Tuzar, Z.; Konak, C.; Stepanek, P.; Plestil, J.; Kratochvil, P. *Polymer* **1990**, *31*, 2119.
[20] Thiyagarajan, P.; Epperson, J.E.; Crawford, R.K.; Carpenter, J.M.; Klippert, T.E.; Wozniak, D.G. *J. Appl. Crystallogr.* **1997**, *30*, 280.
[21] Kinning, D.J.; Thomas, E.L. *Macromolecules* **1984**, *17*, 1712.
[22] Percus, J.K.; Yevick, G.J. *Phys. Rev.* **1958**, *110*, 1.
[23] Hashimoto, T.; Fujimura, M.; Kawai, H. *Macromolecules* **1980**, *13*, 1660.
[24] Kroschwitz, J.I. *Concise Encyclopedia of Polymer Science and Engineering* , J. Wiley, New York 1990.
[25] Konak, C; Fleischer, G.; Tuzar, Z.; Bansil, R. *J. Polym. Sci B: Polym. Phys.* **2000**, *38*, 1312.
[26] Mortensen, K. *Europhys. Lett.* **1992**, *92*, 599.
[27] Christian, J.W. *The Theory of Transformations in Metals and Alloys.* Part I, Pergamon, New York 1981.
[28] Cahn, J.W. *Acta Metall.* **1956**, *4*, 449.